Solar Flare Activity and Variability of Electric Current Helicity

Kim Jik Su[1,2], Hong-Qi Zhang[1] [*], Kim Jin Song[1,2], Kim Kum Sok[1,2] and Xing-Ming Bao[1]

[1] National Astronomical Observatories, Chinese Academy of Sciences, Beijing 100012
[2] Pyongyang Astronomical Observatory, Academy of Sciences, DPR of Korea

Abstract Recent study using Huairou vector magnetograph data shows that during flare activity, the current helicity exhibits rapid and substantial variations and, in some cases, a recovering phase. We considered various representative the magnetic configurations. First, interacting twisted magnetic flux tubes are analyzed separately for positive, negative and mixed-sign helicity regions. The results show that the helicity during flares decreases in positive-sign, and increases in negative-sign regions. Then, flaring arcade also shows that the magnitude of the helicity decreases after flares. We also investigated current sheets formed by sheared magnetic field and showed that the current helicity (with either positive and negative signs) vanishes after reconnection. The emergence of twisted flux tubes which can trigger flares may be another source of flare-associated variability of current helicity. We demonstrate the relevance of current helicity to the description of flare activity by comparing its variation with that of shear angle in the active region AR 6891.

Key words: Sun: flare — Sun: current helicity — Sun: magnetic shear

1 INTRODUCTION

Recently Bao, Zhang, Ai, and Zhang (1999), using Huairou vector magnetograph data, have shown that the average current helicity $\langle h_c \rangle$ or the current helicity imbalance ρ_h of active regions change rapidly after solar flares. Upon the onset of flares it tends to decrease for a few hours and then to increase again, whereas in some cases the flare promotes an increase in the current helicity. The observations led to the following conclusions: (1) rapid and substantial changes of current helicity distribution in an area probably lead to flare eruption in that area of its vicinity; (2) active regions in which the average current helicity undergoes a significant change show more flare activity than do typical active regions; (3) there is no clear correlation between the peak values of the current helicity and the flare kernels; (4) the rate of variation of current helicity may better characterize the non-potentiality of the active region magnetic

---

[*] E-mail: hzhang@class1.bao.ac.cn

fields — perhaps it can provide us with more information than other parameters such as angular shear or vertical current.

In this paper we investigate typical magnetic configurations of solar active regions and find possible explanations of the above-mentioned variability of current helicity associated with flare activity. Many authors have found observational signatures of non-potentiality of the magnetic structure of active regions in their "angular shear" (Hagyard et al. 1984; Wang 1992; Lü, J.Wang & H. Wang 1993; Ambasta et al. 1993), however, it has become clear more recently that magnetic shear is not a sufficient condition for flares (Chen et al. 1994; Hagyard 1997). Chen et al. presented Huairou vector magnetograph data of six active regions, and showed that only seven of the 20 M-class (or stronger) flares satisfy the flare conditions prescribed by Hagyard et al. (1984) and in some flares the shear increased instead, and this indicates that strong photospheric shear is not necessarily a condition for flares.

Recent observations and theoretical research concerning the preflare energy buildup of active regions and the release of stored energy showed that, while the appearance of stressed or sheared magnetic fields along a localized section of a neutral line on the photosphere may be correlated to some extent with the occurrence of flares, the process of energy buildup taking place more widely over different parts of an active region that are magnetically connected may play a significant role (Heyvaerts & Hagyard 1991; Brown et al. 1994; Mandrini et al. 1995).

The magnetic shear angle along the neutral line is a local characteristic of the active region, and it cannot characterize the more global energy buildup for the great variety of magnetic configurations of active regions. So we must invoke some other global characteristics of representative active regions. Now, the non-potentiality of a magnetic configuration is manifested by its global electric current, so in this work we shall consider the electric current helicity as a suitable measure of the non-potentiality and of flare activity.

As we will see below, the electric current alone cannot characterize sufficiently the possibility of flares either. Moreton and Severny (1963) first pointed out a possible physical connection between concentrations of line-of-sight current and Hα flare kernels. Observations with the Marshall vector magnetograph in Cycle 21 have provided further examples (Lin & Gaizauskas 1986; Hagyard 1988). However, new observations showed clearly that flare-generated electron precipitation is generally located at the periphery of the current distributions (Leka et al. 1993; de la Beaujardiere et al. 1993). The results seem to provide constraints on the relationship between the active region current and flares.

Here we first view flare activity in terms of the current helicity and try to find possible explanations of the observational behavior of the current helicity during flare activity. In the next section, for several magnetic configurations of active regions, a close relation between the flare and current helicity is examined and the observational characteristics of the behavior of the current helicity are interpreted. In Section 3, through an analysis of the vector magnetograms of an active region we emphasize the relevance of the electric current helicity to the description of flare activities. In Section 4, finally we discuss the results obtained.

2 FLARE AND ELECTRIC CURRENT HELICITY

Bao, Zhang, Ai, and Zhang (1999), through an investigation of the evolution of current helicity imbalance $\rho_{\rm h}$ or the average current helicity $\langle h_{\rm c} \rangle$ in four flare-productive active regions (NOAA 6233, 6891, 7321 and 7773), found that these quantities showed rapid and significant changes during flare activities and a tendency to recover (Fig. 1), whereas flare-poor active

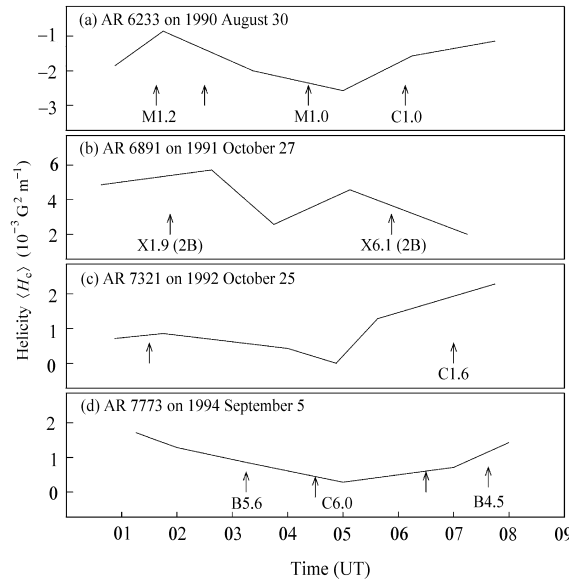regions do not show such significant time variations.

Fig. 1   Variations of the average current helicity of the photospheric magnetic fields as a function of time in four flare-productive active regions (NOAA 6233, 6891, 7321 and 7773). Arrows indicate onset times of flares.

In order to elucidate the significance of the flare-associated variations of current helicity variations, we consider two typical flare-producing magnetic configurations, interacting twisted loop systems and flaring sheared arcades along with the general current sheets formed by the sheared magnetic field and we ascribe the variation of current helicity to the emergence of twisted magnetic flux tubes.

2.1   Interaction of Twisted Flux Tubes

Wang (1994), analyzing vector magnetograms of Huairou Solar Observing Station, found that strong magnetic shear is intrinsically related to emerging flux regions, and that collision of sunspots with opposite polarities almost always takes place between an emerging flux region and some pre-existing fields. Kurokawa (1987) found that only the emergence of twisted magnetic loops produces sheared fields that are correlated with major flares. In the description of the interactions of various emerging and pre-existing magnetic structures, Wang (1994) preferred to use the term "magnetic flux" or "magnetic loop" to "sunspots", and we shall follow this practice here and focus on the interaction of twisted magnetic loops. Akai and Koide (1992), considering various cases of interaction between two twisted magnetic loops, classified θ-reconnection and z-reconnection according to which of the magnetic field components is reconnected, and showed that out of seven possible cases three resulted in θ-reconnection, three in z-reconnection, and one in no reconnection. Figure 2 shows the two topologically different cases of interacting twisted magnetic flux tubes.

In Figure 2 and thereafter we concentrate our attention on the vertical sections of the magnetic loops, and accordingly simplify the drawing near the foot points of the loop, because modern vector magnetograms observed at a single height allow us to compute only the contribution of the vertical current to the current helicity $\mu_0 B_z j_z$. Generally the current helicity density is defined by $h_c = \mu_0(j_x B_x + j_y B_y + j_z B_z)$. However, from now on we will denote only the measurable current helicity $\mu_0 j_z B_z$ by h_c. The panels of the first column correspond to θ-reconnection, those of the second column, to z-reconnection, those of the third column, to θ- and z-reconnections, and those of the fourth column, to no reconnection. The θ-reconnection decreases the total helicity of the two flux tubes because the interaction of two flux tubes with separate initial currents I_1 and I_2 generates a current I_{cs} opposite to the initial currents. This decrease may be simply estimated. For a radius of the flux tubes R and a θ-component magnetic field B_θ, the initial currents are $I_1 = \frac{1}{\mu_0} \int B_\theta \mathrm{d}l = 2\pi R B_\theta/\mu_0 = I_2$ and the total current is $I = I_1 + I_2 = 4\pi R B_\theta/\mu_0$. After reconnection the current is given by $I' = \frac{1}{\mu_0} \int B_\theta \mathrm{d}l = (2\pi R + 4R)B_\theta/\mu_0 < I$, so in the post-flare phase the total helicity is $H'_c = \mu_0 B_z I' < H_c$. Thus, the helicity decreases after the flare: $(\Delta H_c < 0)$.

Reconnection	θ - reconnection	z - reconnection	θ- and z - reconnection	no - reconnection
Pre-flare phase	I_1 ▲ ▲ I_2 ; I_{cs} ; B_z ↑↑↑↑↑ ↑↑↑↑↑ ; $B_z I_1 > 0$, $B_z I_2 > 0$; $H_c > 0$	I_1 ▽ ▲ I_2 ; ↓↓↓↓↓ ↑↑↑↑↑ ; $B_z I_1 > 0$, $B_z I_2 > 0$; $H_c > 0$	I_1 ▲ ▲ I_2 ; I_{cs} ; ↑↑↑↑↑ ↓↓↓↓↓ ; $B_z I_1 > 0$, $B_z I_2 < 0$; $H_c = 0$	I_1 ▲ ▽ I_2 ; ↑↑↑↑↑ ↑↑↑↑↑ ; $B_z I_1 > 0$, $B_z I_2 < 0$; $H_c = 0$
Intermediate state		(a) B_z ↓↓↓ ↑↑↑ ; (b) B_z ↓↓↓↑↑↑	(a) ↑↑↑ ↓↓↓ ; (b)	
Post-flare phase	▲ I' ; $B'_z = B_z$ ↑↑↑↑↑↑↑↑↑↑ ; $I' < I_1 + I_2$; $H'_c = B_z I' < H_c$	I_1 ▽ ▲ I_2 ; $H'_c < H_c$	▲ I' ; $I' < I_1 + I_2$; $H'_c < H_c$	I_1 ▲ ▽ I_2 ; ↑↑↑↑↑ ↑↑↑↑↑ ; $H'_c = H_c$
$\Delta H_c = H'_c - H_c$	< 0	< 0	$= 0$	$= 0$

Fig. 2 θ-, z- and $\theta - z$-reconnections of two twisted magnetic flux tubes.

The panels in the second column corresponding to z-reconnection also show a decrease in total helicity. Note that the first and second columns are only for the case of positive helicity. The case of negative helicity is the same, differing only by the sign, so the helicity increases after the reconnection $(\Delta H_c > 0)$. The third column corresponding to θ- and z-reconnections shows eventual complete cancellation of the z-component of the field as in the second column, so the

total helicity vanishes after the reconnection. However, although the separate flux tubes before reconnection have nonzero helicities, the total helicity is zero if the flux tubes are identical in size and in absolute magnitude of the line-of-sight field component. After reconnection the vertical component of the field vanishes, so there is no change of the total helicity. The fourth column for no reconnection is trivial.

Based on the above consideration we may picture the interacting coronal loops as in Figures 3, 4, 5, respectively for positive, negative and mixed-sign-helicity regions, according to the current-helicity-sign-rule (Seehafer 1990; Pevtsov, Canfield & Metcalt 1996; Bao & Zhang 1998). In the positive helicity region all the cases show a decrease of the helicity, whereas the region of negative helicity shows an increase of the helicity after reconnection. The mixed-helicity-region shows no change of the helicity at all.
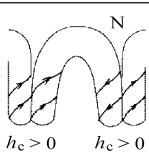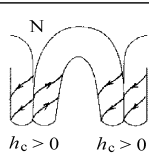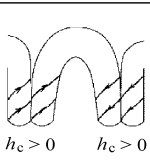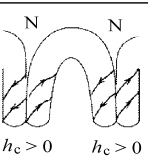

Fig. 3 Interaction of flux tubes in positive helicity region.

Fig. 4 Interaction of flux tubes in negative helicity region.
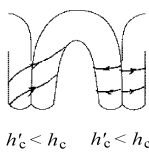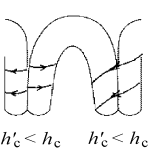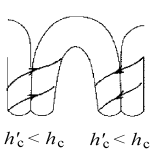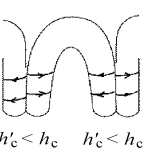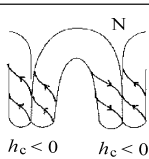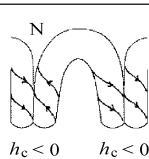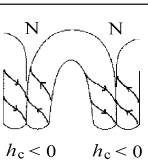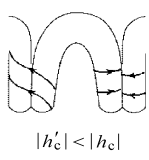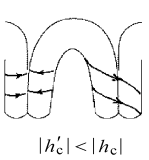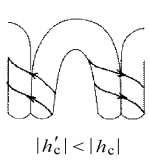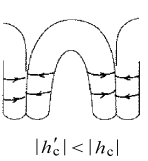
	Mixed-sign-helicity region			
pre-flare phase	$\langle h_c \rangle = 0$ $\langle h_c \rangle = 0$	$\langle h_c \rangle = 0$ $\langle h_c \rangle = 0$	$\langle h_c \rangle = 0$ $\langle h_c \rangle = 0$	$\langle h_c \rangle = 0$ $\langle h_c \rangle = 0$
post-flare phase	$\langle h'_c \rangle = 0$ $\langle h'_c \rangle = 0$	$\langle h'_c \rangle = 0$ $\langle h'_c \rangle = 0$	$\langle h'_c \rangle = 0$ $\langle h'_c \rangle = 0$	$\langle h'_c \rangle = 0$ $\langle h'_c \rangle = 0$
$\Delta \langle h_c \rangle$	$= \langle h'_c \rangle - \langle h_c \rangle$	$= 0$	$= 0$	$= 0$

Fig. 5   Interaction of flux tubes in mixed-sign-helicity region.

Let us now estimate the change of the helicity density (h_c) for reasonable values of the two interacting twisted flux tubes (see θ-reconnection of Fig. 2). The current density of two identical flux tubes before reconnection is given by

$$j = \frac{I_1 + I_2}{2\pi \mu_0 R^2} = \frac{2 B_\theta}{\mu_0 R}.$$

After reconnection it becomes

$$j' \leq \frac{2(\pi + 2) R B_\theta}{\mu_0 (\pi R^2 + 4 R^2)} = \frac{2(\pi + 2) B_\theta}{(\pi + 4) \mu_0 R}.$$

So $j' < j$. On the other hand, from the equality $(\pi^2 R^2 + 4 R^2) B'_z = 2\pi R^2 B_z$, we obtain $B'_z \approx 0.9 B_z < B_z$. If we assume $B'_z \approx B_z$ the current helicity is given by

$$\Delta h_c = \mu_0 (j' B'_z - j B_z) \approx \mu_0 (j' - j) B_z \approx -\frac{4 B_\theta B_z}{(\pi + 4) R} < 0.$$

For typical flux tubes in active regions $R \approx 5 \times 10^7\,\mathrm{m}$, $B_z \approx 300\,\mathrm{G}$ and $B_\theta \approx 300\,\mathrm{G}$, we obtain $\Delta h_c \approx -1.1 \times 10^{-3}\,\mathrm{G^2 m^{-1}}$. This is in good agreement with the observational result, $|h_c| \approx (2-4) \times 10^{-3}\,\mathrm{G^2\,m^{-1}}$ (Bao et al. 1999).

So far we have considered only the interaction of two magnetic tubes; in fact, however, a number of emerging flux tubes may interact in emerging flux regions (Figure 6). The coalescence of three flux tubes generates three additional downward currents $3 I_{cs}$ at the three interfaces, decreasing the total current $(3 I_1 - 3 I_{cs})$ and hence the total helicity. Closely packed seven flux tubes generate 12 additional currents $12\, I_{cs}$, and the the total current decreases even more, by $(7 I_1 - 12 I_{cs})$.

A quite common characteristic of the variation of the current helicity is that the variation associated with flares shows a recovering phase (Bao et al. 1998; Deng et al. 2001). This

appealing behavior of the current helicity seems to have its root in two different phenomena: magnetic relaxation and emergence of new magnetic fluxes.
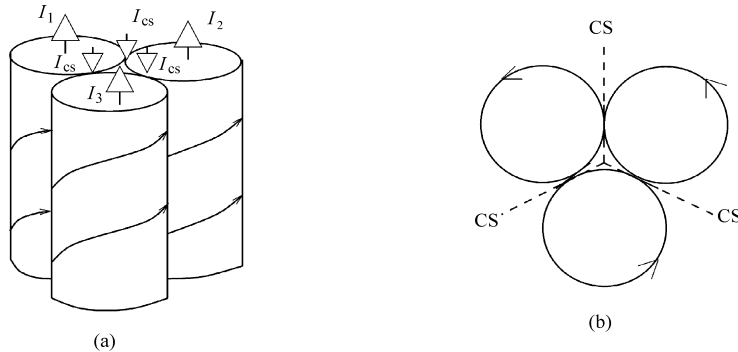

Fig. 6 Interaction of three positive helicity flux tubes. (a) view of top-side; (b) view of top of the current sheet.

Parker (1972) was the first to prove an important theorem according to which a large scale magnetic field possesses a hydrostatic equilibrium only if the pattern of small scale variations is uniform along the large scale field. After a flare, a non-uniform distribution of small scale variation of magnetic field may be formed, which makes the distribution of the current helicity uniform. In general, the relaxation of a non-uniform (stressed) magnetic configurations after reconnection in the flaring site is likely to be an inevitable process and naturally builds the current helicity anew.

The emergence of new twisted magnetic flux tubes and the transportation of magnetic energy and current helicity into the corona may be another source of recovering the helicity and seems to be responsible for the helicity build-up (Deng et al. 2001).

2.2 Flaring Arcades

Most of major flares are believed to be associated with non-equilibrium, sheared arcades (Priest 1981; Low & Nakagawa 1975; Low 1977; Martens & Kuin 1989).

We choose a simple model of sheared arcade as follows:

$$B_x = \frac{lB_0}{k} \cos kx e^{-lz}, \qquad B_y = \frac{\alpha B_0}{k} \cos kx e^{-lz}, \qquad B_z = -B_0 \sin kx e^{-lz} , \qquad (1)$$

where α is the force free factor and $l^2 = k^2 - \alpha^2$. This configuration is force free, and is characterized by an arcade-shear angle $\gamma = \arctan\left(\frac{k^2}{l^2} - 1\right)^{\frac{1}{2}}$. In this model, the neutral line coincides with the y-axis and the z-axis is directed upward. The footpoints of the arcade extend in the direction of the x-axis from $-\frac{\pi}{2k}$ to $\frac{\pi}{2k}$.

There is no loss of ideal-MHD equilibrium or stability in this model as the footpoints are displaced, and it is thought that a simply connected, infinitely long, two-dimensional arcade always remains in a stable equilibrium as the footpoints are sheared (Finn & Chen 1990). However, a sufficiently sheared arcade ($\gamma \to \frac{\pi}{2}, l \to 0$) must be in a strongly stressed state and this state may be representative of pre-flare magnetic stress. An arcade model a little different from the above was used to show the flare eruption of the magnetic configuration on one occasion (Low & Nakagawa 1975; Low 1977).

The global current helicity per unit length in the direction of the y-axis and from the photosphere level to the height $\frac{1}{l}$, calculated by the arcade model (1), is given by

$$H_{\rm c} = \frac{\pi \alpha B_0^2}{4kl}(1 - e^{-2}) = \frac{\pi \sqrt{k^2 - l^2}}{4kl} B_0^2 (1 - e^{-2}). \qquad (2)$$

In the potential configuration ($l = k$), the helicity vanishes, but in a highly stressed state ($l \to 0$), the current helicity becomes very large. Let us estimate the change of helicity using Equation (2). The volume of unit length along the y-axis is $\frac{\pi}{kl}$, so $h_{\rm c} \approx \alpha B_0^2/4$. Substituting the relevant values $B_0 \approx 500\,{\rm G}, \alpha \approx 10^{-7}\,{\rm m}^{-1}$ (Zhang et al. 2002) gives $h_{\rm c} \approx 6 \times 10^{-3}\,{\rm G}^2\,{\rm m}^{-1}$. The active regions mentioned above show an average change of helicity of $(2-4) \times 10^{-3}\,{\rm G}^2\,{\rm m}^{-1}$ (Bao et al. 1999) which is in good agreement with the above result from the model. The fact that a sheared arcade has a positive helicity may also be checked for a number of various similar arcade models. However, this does not exclude the possibility of a proper arcade model having a negative helicity. Restricting our consideration to the above model, we find the current helicity would decrease after flare eruption.

For the sake of simplicity in describing the flare activity of the magnetic arcade, we have excluded the environment of the arcade, in particular, the complicated structure of the above arcade, and we assume that the major contribution to the helicity is due to the arcade. However, since after flare eruption the formation of the post-flare loops and a new alignment of the post-flare magnetic configuration cannot be treated properly without considering the connection between the arcade and its environment, our consideration above may be over-simplified.

2.3 Flaring Current Sheet

Formation of current sheets in stressed and sheared magnetic configuration is generally recognised as being important during flare activity. Two such current sheets are presented in Figure 7. The upper panels depict two cases of opposite helicity, and the lower panels show
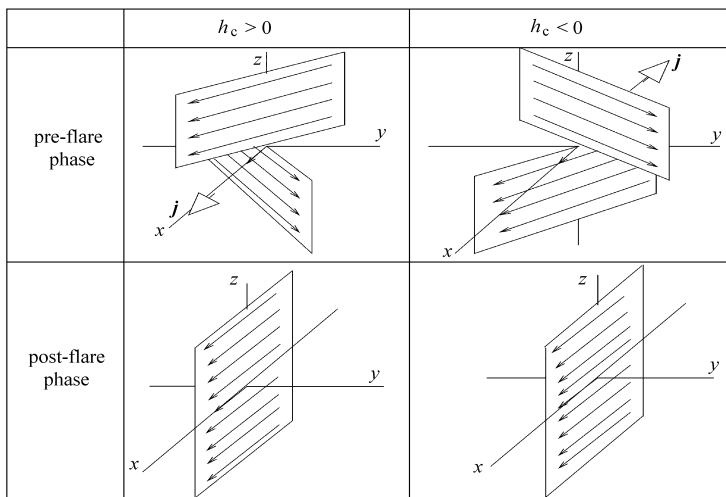

Fig. 7   Change of current helicity in general current sheets through reconnection.

the patterns after reconnection. After reconnection, the helicity of the current sheets vanishes in both cases, this means that the helicity of current sheet either increases or decreases during flare reconnection.

However, the importance of the separate current sheet in global helicity change is doubtful because the current sheets are believed to be very thin (Priest & Forbes 2000). It follows that the modern spatial resolution of vector magnetograms may be insufficient to reveal such a minute structure in the helicity change even though the total variation is large.

2.4 Emergence of Pre-twisted Magnetic Flux Tubes

The emergence of pre-twisted magnetic flux tubes, which can trigger the flare, may be another source of flare-associated variability of the current helicity. Recent observations showed many cases where the flare and related activation of loops are closely linked with the emergence of twisted flux tubes (Kurokawa 1987; Wang 1994; Deng et al. 2001). Leka et al. (1996) analyzed Yohkoh X-ray images, H_α data and vector magnetograms for an active region in which new magnetic bipoles are rapidly emerging and they concluded that emerging magnetic flux appeared at solar surface carrying electric current. They showed that the bipoles are all co-spatial with significant vertical current densities, and that these currents appear in the photosphere during the emergence of the bipoles.

Theoretical support for the emergence of current-carrying flux tubes was provided by Melrose (1995). He argued that the observed currents in the photosphere cannot be generated by shearing or other motions on an unsheared field near the photosphere and the observed shearing of coronal magnetic structures is caused by the emergence of current-carrying magnetic fields.

These observational and theoretical evidences indicate that the flares which occur through the interaction of emerging with pre-existing magnetic fluxes must be accompanied by variation of current helicity carried by the emerging flux tubes. This must be another source of the variability of the current helicity associated with flare activity.

3 RELEVANCE OF THE CONCEPT OF CURRENT HELICITY FOR THE DESCRIPTION OF FLARE ACTIVITY

As mentioned above, it has become clear that angular shear is not a sufficient condition for flares (Chen et al. 1994; Hagyard 1997). We argue that the global characteristics of current helicity (e.g., helicity imbalance ρ_h or average current helicity $\langle h_c \rangle$) for a given active region may be one of suitable signatures of flare activity. By this we mean that the flare activity manifests surely through a variation of the current helicity (Bao et al. 1999).

Chen et al. (1994) analyzed the behavior of angular shear along the neutral line of a 3B flare occurred on 27 October, 1991 in AR 6891 and found that there is no detectable change of angular shear during the flare activity. Bao et al. (1999), however, found a significant change of the average current helicity for the same event, amounted to $(2-4) \times 10^{-3}\,\mathrm{G^2\,m^{-1}}$ over the noise level.

In Section 2.1, we analyzed various cases of interacting loops and showed that θ-reconnection and z-reconnection give rise to a number of field line patterns. If the vertical (line-of-sight) field component of two interacting columns is oppositely directed, then a neutral line will be formed between them (the lines labelled N in Fig. 3, 4, 5). However, the "shear angle" caused by the θ-component of the field does not show any change in Fig. 3 or Fig. 4 in spite of the reconnection and relaxation, whereas the total helicity changes in all cases. On the other hand, Fig. 5 shows the change of angular shear $\triangle\theta \approx 90°$ while the current helicity shows almost no change. This

means that the angular shear may serve as a measure for characterizing flare activity in mixed sign regions. However, such regions account for only about 20% of all active regions (Zhang et al. 2002). The definite part where the shear angle shows little change may correspond to the cases of Figs. 3 and 4 for interacting twisted magnetic tubes. Zhang and Bao (1998) showed that most of the regions that produce powerful flares exhibit strong current helicity (e.g., AR 5395 and AR 6659), and the helicity is an important index of the reserve magnetic energy in the region. The examples in the previous section provide affirmative evidence for the high current helicity buildup before flares.

4 DISCUSSION AND CONCLUSIONS

The observations and analyses mentioned above make us believe that rapid and substantial changes of the current helicity distributions in active regions probably cause flare eruptions and the rate of variation of the current helicity may provide a better measure of non-potentiality of the local magnetic field.

In order to find a satisfactory explanation of the observational results, we analyzed the interaction of twisted magnetic flux tubes, the relaxation of a simple magnetic arcade and the reconnecting current sheets. Especial emphasis is on the interaction of twisted loops, because recent observations reveal the importance of the emergence of pre-twisted fields in the formation of active centers. Wang (1994) has explicitly shown a term associated with the emergence of twisted fields in his shear-generating equation. Kurokawa (1987) found in a study of six active regions that only the emergence of twisted magnetic loops produces sheared field that is correlated with major flares. As shown in Section 2.4, the emergence of pre-twisted magnetic flux tubes carrying current helicity causes the current helicity to increase in size, and then the interaction of the emerged flux with pre-existing magnetic flux causes further changes in the helicity.

Our analyses show that all cases of interacting flux tubes we considered exhibit either a decrease (Fig. 3) or an increase (Fig. 4) in the current helicity, except for mixed-sign regions. This means that energy relaxation relates properly to helicity relaxation. In a mixed-sign helicity region the helicities of separate flux tubes are changed, but the average helicity density $\langle h_c \rangle$ does not change throughout the flare activity. Accordingly, we may conclude that for mixed-sign helicity regions we should preferably use the local helicity density h_c rather than the average density $\langle h_c \rangle$ to characterize the non-potentiality of the magnetic configuration. In comparison with the average helicity $\langle h_c \rangle$ for mixed-sign-helicity region, the angular shear is better in characterizing the non-potentiality.

While the analysis of magnetic arcade using a greatly simplified model does show a significant decreases of the helicity during flare activity, this results is insufficient for a definite conclusion and one has to work out a detailed model for deriving the global helicity taking into account of the whole environment of the arcade. The contribution to the helicity variation by current sheets seems to be negligible because their minute spatial scale makes it impossible to detect any change of their helicity. However, if we could identify some large part of the current sheet, then its contribution could be set off against other more global contributions; after all, current sheets are believed to be the locus of the most intense activity and/or change of helicity during flares.

Summing up the results we conclude that in the interacting flux tubes the current helicity is an intrinsically reasonable quantity for detecting almost all the variations associated with flare

activity, and this means that the helicity may be a measure of the non-potentiality of a given magnetic structure. Further observations would be expected to check up the time-behavior of the current helicity in various patterns of magnetic configuration, especially in various cases of twisted pre-existing flux tube interacting with twisted emerging flux and in the loci that are thought to be an arcade.

References

Ambasta A., Hagyard M., West E. A., 1993, Solar Phys., 148, 277
Bao S., Zhang H., 1998, ApJ, 496, L43
Bao S., Zhang H., Ai G., Zhang M., 1999, A&AS, 139, 311
Brown J. C., Correira E., Farnik F. et al., 1994, Solar Phys., 153, 19
Chen J., Wang H., Zirin H., Ai G., 1994, Solar Phys., 154, 261
de la Beaujardiere, Canfield R. C., Leka K. D., 1993, ApJ, 411, 378
Deng Y., Wang J., Yan Y., Zhang J., 2001, Solar Phys., in press
Finn J. M., Chen J., 1990, ApJ, 349, 345
Hagyard M., 1988, Solar Phys., 115, 107
Hagyard M., 1987, in : G. Heckman, K. Marubash, M. A. Shea, D. F. Smart, R. Thompson, Solar - Terrestrial
    Prediction, Vol. 5, RWC Tokyo, Hiraiso STR Center, 527
Hagyard M., Smith J. B., Teuber D., West E. A., 1984, Solar Phys., 91, 115
Heyvaerts J., Hagyard M., In: B. Schmieder, E.Priest, eds., Dynamics of Solar Flares, 1
Kurokawa H., 1987, Solar Phys., 113, 259
Kuzanyan K., Bao S., Zhang H., 2000, Solar Phys., 191, 231
Leka K. D. et al., ApJ., 411, 370
Lin Y., Gaizauskas V., 1986, Solar Phys, 109, 81
Low B. C., 1977, ApJ., 212, 234
Low B. C., Nakagawa Y., 1975, ApJ, 199, 237
Lü Y., Wang J., Wang H., 1993, Solar Phys., 148, 119
Mandrini C. H. et al., 1995, A&A, 303, 927
Martens P. C. H., Kuin N. P. M., Solar Phys., 122, 263
Melose D., 1995, ApJ, 451, 391
Moffatt H. K., 1985, J. Fluid Mech., 159, 359
Moreton G. E., Severny A. B., 1963, Solar Phys., 3, 282
Parker E. N., 1972, ApJ, 174, 499
Pevtsov A. A., Canfield R. C., Metcalf T. R., 1995, ApJ, 440, L109
Priest E., 1981, Solar Magnetohydrodynamics, Dordrecht: Reidel
Priest E., 2000, Magnetic Reconnection, Cambridge: Cambridge Univ. Press
Sakai J., Koide S., 1992, Solar Phys., 142, 399
Seehafer N., 1990, Solar Phys., 125, 219
Wang H., 1992, Solar Phys., 140, 85
Wang J., 1994, Solar Phys., 155, 285
Zhang H., Bao S., 1998, A&A, 339, 880
Zhang H., Bao S., 1999, ApJ, 519, 876
Zhang H., Bao S., Kuzanyan K. M., 2000, Astronomy Report, in press